Int. J. Electrochem. Sci., 14 **(2019)** 575 – 584, doi: 10.20964/2019.01.03

International Journal of ELECTROCHEMICAL SCIENCE
www.electrochemsci.org

Short Communication

Magnetron Sputtering of Gadolinium-doped Ceria Electrolyte for Intermediate Temperature Solid Oxide Fuel Cells

Andrey A. Solovyev[*], *Sergey V. Rabotkin, Anna V. Shipilova, Igor V. Ionov*

Laboratory of Applied Electronics, Institute of High Current Electronics, Siberian Branch of the Russian Academy of Sciences, Tomsk, Russia
[*]E-mail: andrewsol@mail.ru

Received: 29 August 2018 / *Accepted:* 25 October 2018 / *Published:* 30 November 2018

Reactive magnetron sputtering was used for deposition of thin Gd-doped ceria (GDC) films on porous NiO–YSZ (nickel oxide–yttria stabilized zirconia) substrates. X-ray diffraction and scanning electron microscopy were used to study the effect of cathode peak power density on 5–7 μm-thick film's microstructure and surface morphology. It was shown that peak power density (changed from 52 to 490 W/cm^2) has an effect on the crystallite size, microstrains and texture coefficient of the GDC electrolyte. Increasing peak power density suppresses the columnar structure of deposited films and leads to formation of more continuous and denser films. As a result, anode-supported single cells with sputtered at room temperature GDC electrolyte were fabricated and demonstrated maximum power density of 1.07 W/cm^2 at 750 °C.

Keywords: Gadolinium-doped ceria, Magnetron sputtering, SOFC, Microstructure, Electrochemical performance.

1. INTRODUCTION

CeO_2-based electrolytes are considered as an alternative to zirconia-based electrolytes for intermediate temperature solid oxide fuel cells (IT-SOFC), because they have higher ionic conductivity at 500–700 °C and their cost is lower in comparison with $LaGaO_3$-based electrolytes [1,2]. Sm^{3+}- and Gd^{3+}-doped ceria possess the maximum conductivity among ceria-based ceramics [2]. In addition, fabrication of thin film electrolyte also reduces the resistance to ionic migration, resulting in high performance of SOFCs at relatively low temperatures [3,4]. Operation at low temperatures is preferable because arises opportunity to use cheaper stainless steels for interconnectors, the mutual diffusion and thermal mismatch between electrolyte and electrodes are reduced [5]. Thin-film CeO_2-based electrolytes

are usually fabricated by physical and chemical vapor deposition techniques, such as electron beam evaporation [6], pulsed laser ablation [7], sputtering [8], spray pyrolysis [9], metal-organic vapor deposition [10] and others. It is considered that relatively low deposition rates and high equipment cost are characteristic of the vacuum deposition methods in comparison with traditional methods of ceramic layers formation (screen printing, electrophoretic deposition, tape calendering, tape casting) [11]. Despite this, vacuum methods have a number of unique advantages, which are not typical of traditional methods. For example, very thin, fully dense layers may be fabricated at low temperatures.

In order to obtain oxide films of reproducible composition radio-frequency (rf) magnetron sputtering of ceramic targets is usually used [12]. But this method has such disadvantages as very low deposition rates; expensive power supply and additional impedance matching circuitry; the difficulty of scaling onto large-area substrates. Reactive magnetron sputtering is often used technique for deposition of dense gadolinium-doped ceria electrolyte. Although this method also has disadvantages, such as discharge hysteresis and low deposition rate in oxide sputtering mode [13]. For instance, GDC often used as barrier layer between the strontium-doped lanthanum cobalt oxide cathode and zirconia-based electrolyte [14,15]. Fonseca *et al.* [14] have shown that magnetron sputtering of GDC layers with bias applied to the substrate allows obtaining microstructures denser than those obtained without bias. This is result in increasing of electrochemical properties of fuel cells. It has been shown that the combination of substrate heating and the substrate bias is an effective method of the GDC layers microstructure controlling. However, there is not enough information about the influence of plasma ionization degree on the properties of sputtered GDC films. In sputtering processes, high degree of ionization of sputtered particles has been shown to positively influence the deposition of films with dense structure [16]. Therefore, high power impulse magnetron sputtering (HiPIMS) has attracted a great deal of attention because the sputtered material is highly ionized and high plasma concentrations (in the order of 10^{12}–10^{13} cm^{-3}) are observed [17,18]. Recently, Sønderby *et al.* [19] have demonstrated that application of HiPIMS allows producing dense YSZ electrolyte films on porous anode substrates.

In the present work, thin films of Gd-doped ceria electrolyte were deposited by reactive pulsed magnetron sputtering in pulsed-DC and HiPIMS regimes at room temperature on porous anode substrates. The aim of this work was to study the influence of cathode peak power density on the thin films microstructure, crystallite size and texture, as well as performance of single cells with thin-film electrolyte.

2. EXPERIMENTAL

$Ce_{0.9}Gd_{0.1}O_{1.95}$ thin films were deposited by pulsed magnetron sputtering on the commercial NiO–YSZ anodes (SOFCMAN, China). Before the deposition, the substrates with a diameter of 20 mm were ultrasonically cleaned sequentially in pure isopropyl alcohol, acetone and distilled water. Subsequent cleaning of the substrates was performed in vacuum chamber by sputtering using an ion source with closed electron drift (produced by Institute of high current electronics, Russia). Ion treatment lasted 10 min at a discharge voltage of 2 kV and discharge current of 100 mA. The residual pressure in the vacuum chamber was $1.0 \cdot 10^{-3}$ Pa, while working pressure was 0.25 Pa. Argon and oxygen flows

were kept constant at 11 and 4 sccm, respectively. Substrate was located at 8 cm distance over the target. Deposition was performed on the stationary substrate with a constant average discharge power of 1 kW at different peak power densities for metallic Ce-Gd target (90:10 at.%) with a diameter of 100 mm. Magnetron was connected to APEL-M-5PDC or APEL-M-HIPIMS power supply (Applied Electronics, Ltd.) to work in pulsed-DC or HiPIMS mode, respectively. Before the deposition series, the dependence of discharge voltage on oxygen flow rate (voltage hysteresis loop) for the sputtering system was measured. The GDC films were obtained in the transition mode of sputtering. In this mode, located between the metallic and oxide mode, high deposition rate and stoichiometric films are observed. In order to study the influence of deposition parameters on the properties of sputtered GDC films, three sets of depositions were performed, the parameters of which are given in Table 1. Samples obtained in these three regimes, are referred to hereafter as S1, S2 and S3, respectively. As the repetition frequency is decreased from 100 to 2.5 kHz, the pulse duration is increased from 10 to 50 μs in order to keep the same time-averaged effective power (1 kW). Respectively, the peak power density and peak discharge current increased from 52 W/cm^2 to 490 W/cm^2 and from 8 to 80 A. The deposition time was chosen in such a way to form films with the thicknesses of about 5–7 μm. All depositions were made at room temperature. But the actual deposition temperature of GDC was far higher than room temperature due to substrate heating by the bombarded Ce/Gd/O atoms, but did not exceed 100-200 °C.

Table 1. Deposition parameters.

Sample	Power density, W/cm^2	Frequency, kHz	Pulse duration, μs	Discharge voltage, V	Peak discharge current, A	Deposition rate, μm/h
S1	52	100	10	370	8	4.8
S2	100	40	12	320	18	4.5
S3	490	2.5	50	350	80	3.6

Current and voltage waveforms (pulse shape, voltage and current amplitude) were measured by a Hioki 2006 current probe and a Hoden H-9258R voltage probe, respectively, and fixed by a digital oscilloscope (LeCroy WA 1002). A spectrometer (AvaSpec-2048USB2) was used for registration of plasma radiation from the magnetron discharge in the range of 237–792 nm with a spectral resolution 0.7 nm. The optical emission spectroscopy (OES) signal was collected perpendicularly to the magnetron-substrate axis by an optical fiber. The spectra were taken at a distance of 30 mm from the target (the time of integration was equal to 100 ms).

The morphological and structural characterizations of deposited GDC films were studied using SEM (FEI Quanta 200 3D) and XRD (Shimadzu XRD 6000) with $Cu_{K\alpha}$ radiation source in grazing incidence geometry, respectively. The Scherrer formula was used to estimate crystallites size. A texture coefficient *R* [13] was used to quantify the XRD results. It was defined as the ratio of the intensities of the largest peak to the sum of the intensities of all peaks. As the diffraction pattern contains (111), (200), (220), (311) peaks, the coefficient *R* of the most intense (111) peak is:

$$R_{111} = I_{111}/(I_{111} + I_{200} + I_{220} + I_{311}).$$

The value R=1 means preferred (111) orientation, and R=0.57 corresponds to the random orientation.

$La_{0.6}Sr_{0.4}CoO_3$ (LSC) cathode (KCERACELL CO., Korea) was screen printed onto the GDC electrolyte and fired *in situ* during the cell test start-up. Thickness of sintered cathode was about 60 μm. The active area of the single cells was 10×10 mm. Electrochemical investigations were performed in testing setup [20] in the temperature interval of 600–750 °C at constant supply of dry hydrogen to the anode (150 ml/min) and air (400 ml/min) to the cathode. Glass sealant was used to obtain gas tightness. For all single cells with electrolyte deposited in different regimes, at least two identic cells were tested.

3. RESULTS AND DISCUSSION

In order to understand plasma processes taking place in particular deposition regimes, it is necessary to use plasma diagnostics. Optical emission spectroscopy allows investigating the variations of ionization degree between the different sputtering regimes. Fig. 1 demonstrates the optical emission spectra of Ce and Ar neutrals and ions measured during reactive pulsed magnetron sputtering of Ce-Gd target at different peak power densities. Neutral and ionic Ar (Ar^0: 763.5 nm, Ar^+: 480.6 nm) and Ce (Ce^0: 500.91 nm, Ce^+: 418.66 nm) peaks were selected for comparison the degree of ionization in the different sputtering regimes. The intensity ratios of ionic to neutral species were shown in Table 2.

Table 2. The intensity ratio of the ionized and neutral emission lines of Ar and Ce under different conditions.

Peak power density P, W/cm^2	Ar^+ / Ar^0	Ce^+ / Ce^0
52	0.18	0.8
100	0.26	0.7
490	1.71	2.08

As can be seen in the table and Fig. 1, sputtering in HiPIMS regime with peak power density of 490 W/cm^2 allows obtaining plasma with a noticeably higher ionization degree than in pulsed-DC regime with peak power density of 52 and 100 W/cm^2, because the ionization degree of both Ar and Ce increases with the power density increasing. The plasma produced in pulsed-DC regime is composed basically of argon neutrals and a small amount of cerium neutrals and ions. Ar^0 peaks are mainly located in the wavelength region 700–780 nm. In HiPIMS regime the intensity of the Ar^0 lines in this region decreases, but the intensity of the Ce^+ and Ar^+ lines in the region of 400–550 nm sharply increases. Neither O nor O_2 pronounced emission lines were observed in the spectra because the intensity of these lines is very small in comparison with the lines of argon.

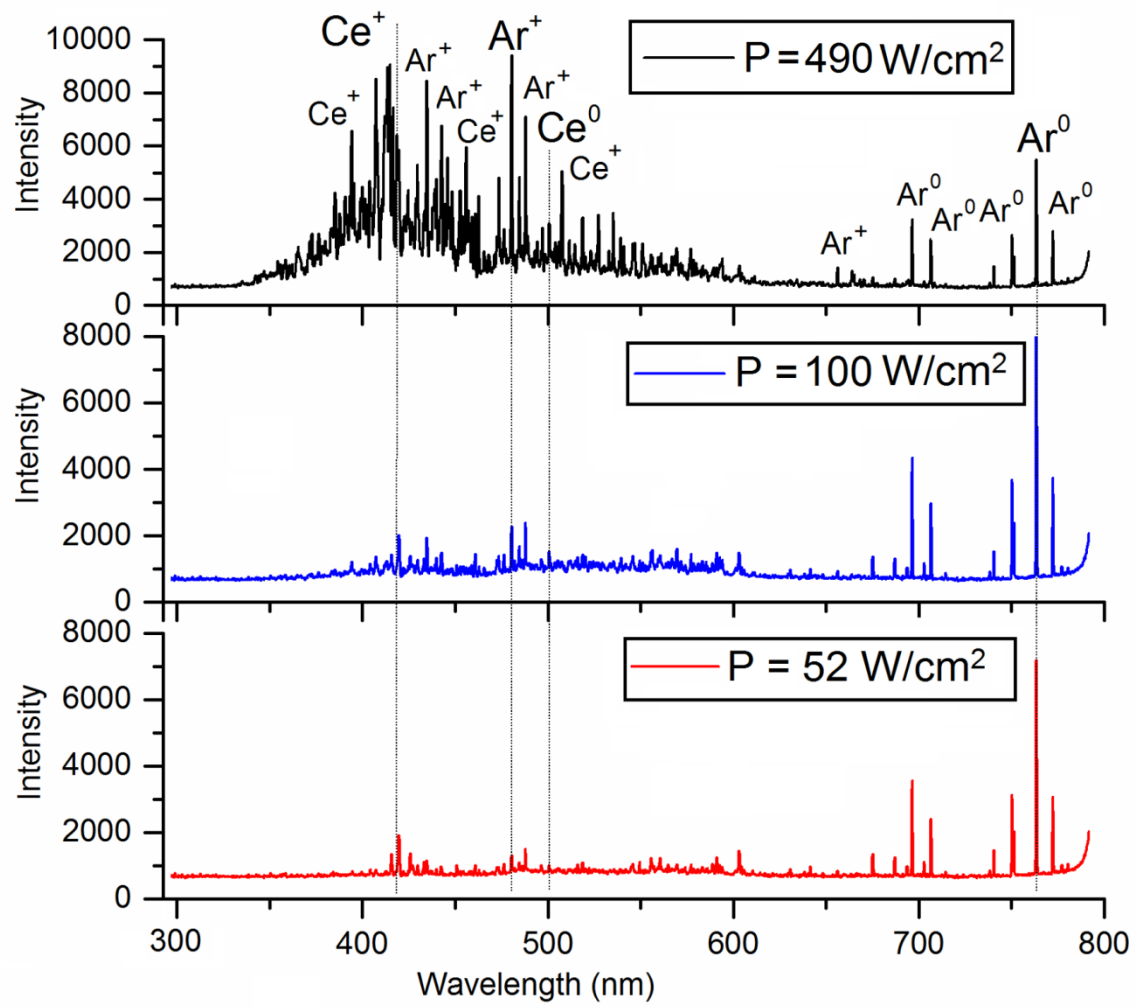

Figure 1. Plasma emission spectra during the magnetron deposition of GDC films at different peak power densities.

Owing to the increase in the degree of ionization, the deposition rate of the films in the HiPIMS regime decreases as is often observed (Table 1). This is one of the drawbacks of HiPIMS regime, because part of the sputtered material is partially ionized and returns back to the target under the influence of an electric field [19].

Fig. 2 shows the X-ray diffraction patterns of as-deposited GDC films. The results of XRD analysis of as-deposited GDC films were compared with JCPDS-PDF no. 75-0162 to confirm the individual phase. All peaks in the diffraction patterns are indexed as GDC. This confirms formation of films without any undesirable phases. The films contains mainly of (111) textured GDC, while minor peaks of (200), (220) and (311) orientation are also observed. This is typical for thin films deposited by magnetron sputtering [13]. Texture coefficient increases with increasing peak power density (Table 3). Dotted lines in Fig 2 show the peak positions from the database. All peaks in obtained XRD patterns are shifted towards smaller angle. This reveals the films are compressively stressed.

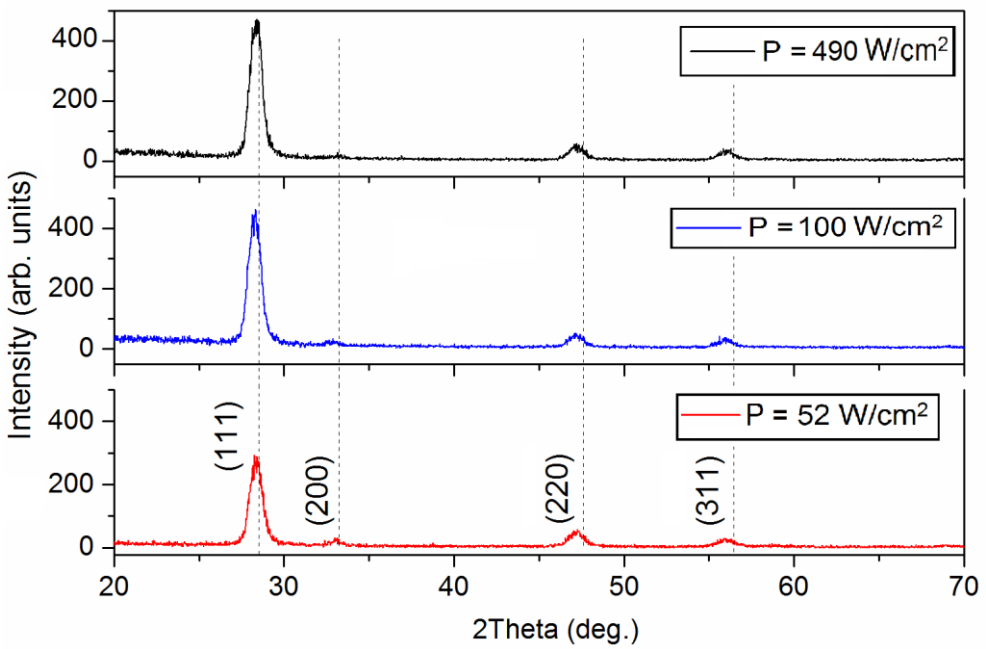

Figure 2. The diffraction patterns of as-deposited GDC films produced on the NiO–YSZ substrate at different peak power densities.

Table 3. XRD analysis results.

Sample	Peak power density P, W/cm^2	Lattice parameter, Å	Crystallite size, nm	Microstrain $\Delta d/d \times 10^{-3}$	Texture coefficient R_{111}
S1	52	a = 5.4057	9	3.8	0.73
S2	100	a = 5.3942	10	3.4	0.81
S3	490	a = 5.4036	11	3.2	0.81

Crystallites size was calculated using the Scherrer formula. Crystallites increased from 9 nm to 11 nm with peak power density increasing (Table 3). However, the microstrains ($\varepsilon_0 = \Delta d/d$) are decreased from 3.8×10^{-3} at P = 52 W/cm^2 to above 3.2×10^{-3} at P = 490 W/cm^2. Previous studies have shown the crystallites size has an impact on the ionic conductivity [21] and has been investigated as a way of increasing ionic conductivity. Jung *et al.* [21] shown that YSZ thin films with nanocrystalline structure demonstrate unpredicted improvement in conductivity in contrast with the microcrystalline material. Nevertheless, the influence of grain size on conductivity is still discussed, because some dispersion is observed in the reported data. Studies of strain-induced fast ion conduction have shown that stresses in films can affect their conductivity. A small tensile stress could increase the conductivity [22,23], but compressive stress leads to a decrease in conductivity [24].

The XRD diffractograms show that the increase of peak power density improves the texture of GDC thin films. This is indicated by the fact that the (111) peak increases more sharply compared to other diffraction peaks. The (111) orientation in the oxygen ion conductors leads to the best electrical conductivity [25].

The SEM images of as-deposited GDC films cross-section (Samples S1-S3) are shown in Fig. 3. It can be seen, that all deposited layers are rather dense, although a columnar film structure is observed in sample S1. In films deposited at higher power density (100 and 490 W/cm^2), the columnar structure is not visible.

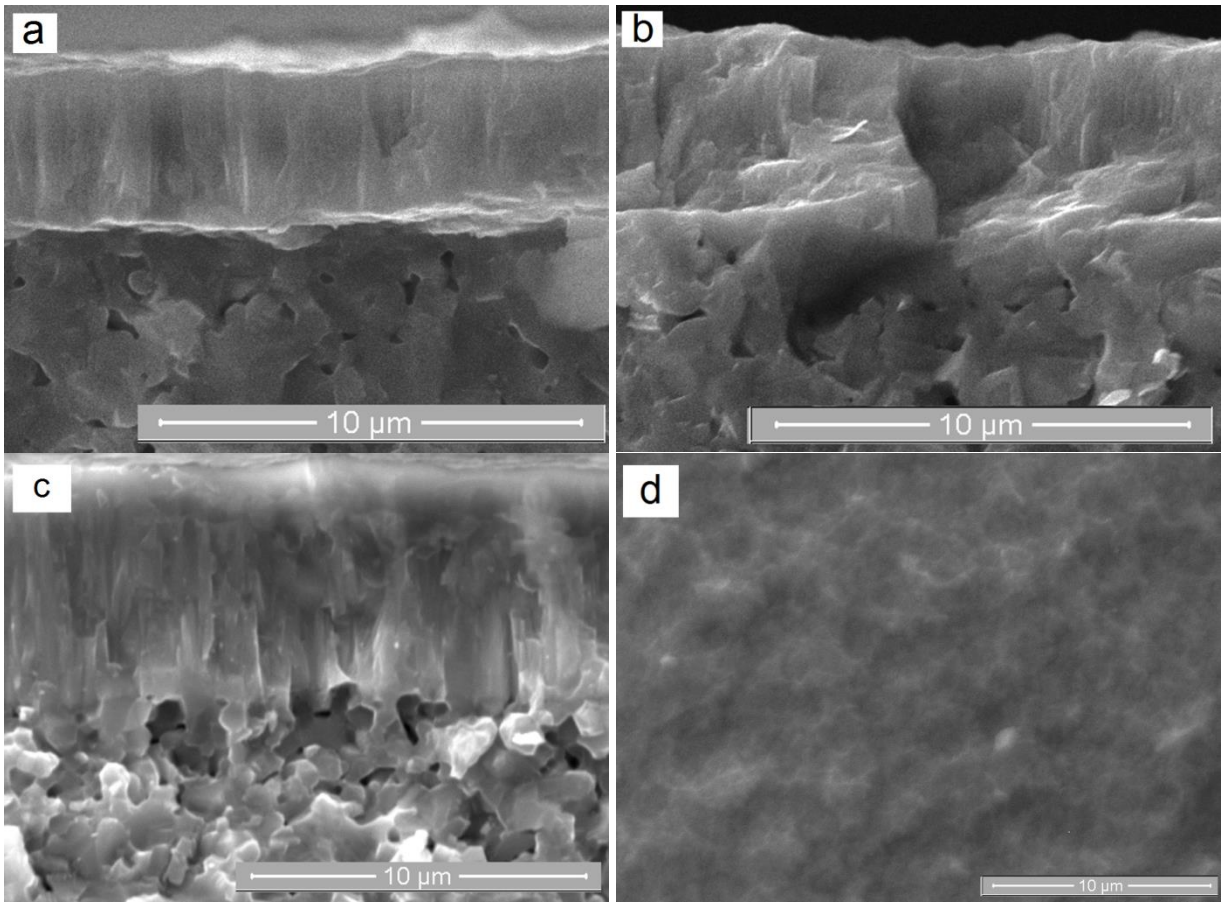

Figure 3. Scanning electron images of the cross section of GDC films deposited onto NiO/YSZ anodes with different peak power densities: (a) 52 W/cm^2, (b) 100 W/cm^2, (c) 490 W/cm^2 and the surface of GDC film deposited at P = 490 W/cm^2.

The columnar structure is typical for sputtered films even on dense flat substrates and arises from islands, formed at the initial stage of film growth [26]. On the porous substrates, the columnar structure of the sputtered films is even more pronounced. In our case when the substrates were not specially heated, microstructure of GDC thin film should correspond to the Zone 1 of the Thornton structure diagram. In the low temperature Zone 1 the ratio between the substrate temperature and the film material melting point (T/T_m) is lower than 0.3. In this zone films usually have a structure with parallel columnar crystallites oriented perpendicular to the substrate [27]. The surface of such films usually has a cauliflower-like structure [28]. In our case all deposited films have rather smooth and dense surfaces without intercolumnar voids even on porous substrates as is shown on Fig. 3, d for Sample S3.

During magnetron sputtering without applying a substrate bias a strong ion mixing process isn't possible. Therefore, the dense microstructure of films deposited at room temperature substrates may be caused by radiation enhanced diffusion. Diffusion coefficient can increase several times due to the fact that the Ar ion bombardment during film deposition creates vacancies. Besides, interaction with plasma could heat the substrate surface to temperatures up to 200 °C, which in turn could increase diffusion [13]. The films grown under higher peak power density become denser, because ion bombardment the growing film increases adatom mobility and leads to the disappearance of voids.

These conclusions are confirmed by the performance of single cells with sputtered GDC electrolyte. Fig. 4 shows typical current-voltage (I-V) characteristics of single cells S2 and S3 with GDC electrolytes sputtered at peak power densities of 100 W/cm^2 and 490 W/cm^2, respectively, measured in the 600–750 °C range. The open circuit voltage (OCV) of cell S1 was between ~0.68 V and ~0.7 V (Fig. 4, a). The maximum power density ranged between 0.25 W/cm^2 at 600 °C and 0.49 W/cm^2 at 750 °C. The I-V curves have convex shape, typical for ceria-based electrolytes [3]. Cells made with YSZ electrolyte have I-V curves with concave shape in low current density region. The observed convex curvature and low OCV values are connected with the mixed ionic–electronic conductivity of GDC [29]. Fig. 4, b shows I-V curves of single cell S3 with GDC electrolyte deposited in HiPIMS regime. The OCV of the cell was slightly higher (0.77–0.8 V). The maximum power density varies between 0.25 W/cm^2 at 600 °C and 1.07 W/cm^2 at 750 °C. The better performance of cell S3 should be attributed to the higher OCV and better microstructure of electrolyte layer deposited in HiPIMS regime.

The measured power densities are within the range of state-of-the-art anode-supported SOFC with GDC electrolyte, reaching ~0.5 W/cm^2 at 650 ºC [9,30]. Usually cells with GDC electrolyte are not tested at temperatures above 650 °C due to a strong decrease in the OCV as a result of reduction of ceria from Ce^{4+} to Ce^{3+} at high temperatures. However, our results show that the use of a GDC electrolyte with an LSC cathode does not lead to a significant decrease in the OCV, and it is possible to achieve a significant increase in cell performance when operating at 750 °C, where YSZ electrolyte is usually used.

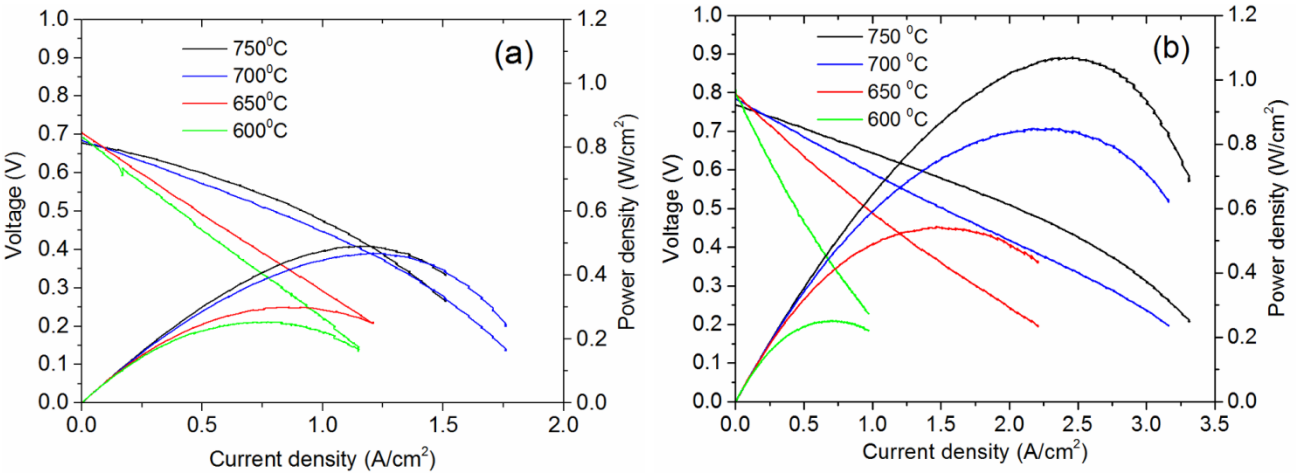

Figure 4. Cell voltage and power density curves measured in the 600–750 °C range for single cells with GDC electrolyte sputtered at peak power density: (a) 100 W/cm^2, (b) 490 W/cm^2.

4. CONCLUSIONS

Plasma during pulsed reactive magnetron sputtering of $Ce_{0.9}Gd_{0.1}O_{1.95}$ films was characterized by optical emission spectroscopy. Emission spectra taken in the transition mode of reactive sputtering revealed distinct changes in plasma composition in the vicinity of the magnetron target when peak power density increases. Increasing of peak power density is followed by a decrease of Ar^0 intensity and an increase of Ce^+, Ce^0 and Ar^+ intensity.

The results show that thin film GDC electrolyte can be obtained on NiO-YSZ anode substrates by reactive magnetron sputtering from a Gd-10 at% Ce alloy target at room temperature without post-treatment in air. The GDC electrolyte films were dense, crack-free, and 5-7 μm in thickness. The peak target power density has a big impact on the microstructure, growth rate and the performance of the electrolyte. Peak power density increasing from 52 to 490 W/cm^2 gradually suppresses the columnar structure of deposited films, promotes formation of a denser films. This was caused by the more intense bombardment of a growing film with ions, which led to increased adatom mobility. Increase of the peak target power density enhances the degree of ionization of both Ar and sputtered material. Therefore, anode-supported single cell with sputtered at higher power density GDC electrolyte has improved electrochemical characteristics. The results show that the peak power density is an important parameter of the sputtering process that improves the quality of Gd-doped ceria electrolyte for IT SOFCs. Maximum power density as high as 1.07 W/cm^2 was measured at 750 °C.

ACKNOWLEDGEMENTS
This work was supported by the Russian Science Foundation (grant No. 17-79-30071).

References

1. T.S. Zhang, J. Ma, L.H. Luo and S.H. Chan, *J. Alloys Compd.*, 422 (2006) 46.
2. V.V. Kharton, F.M.B. Marques and A. Atkinson, *Solid State Ionics*, 174 (2004) 135.
3. H.C. Park and A.V. Virkar, *J. Power Sources*, 186 (2009) 133.
4. C. Ding, H. Lin, K. Sato and T. Hashida, *J. Membr. Sci.*, 350 (2010) 1.
5. J.G. Cheng, S.W. Zha, J. Huang, X.Q. Liu and G.Y. Meng, *Mater. Chem. Phys.*, 78 (2003) 791.
6. G. Laukaitis and J. Dudonis, *J. Alloys Compd.*, 459 (2008) 320.
7. N. Pryds, K. Rodrigo, S. Linderoth and J. Schou, *Appl. Surf. Sci.*, 255 (2009) 5232.
8. C. I. Hernandez, L. Combemale, F. Gao, A. Billard and P. Briois, *ECS Transactions*, 78(1) (2017) 1189.
9. R.P. Reolon, C.M. Halmenschlager, R. Neagu, C.F. Malfatti and C.P. Bergmann, *J. Power Sources*, 261 (2014) 348.
10. H.Z. Song, H.B. Wang, S.W. Zha, D.K. Peng and G.Y. Meng, *Solid State Ionics*, 156 (2003) 249.
11. L.R. Pederson, P. Singh and X.D. Zhou, *Vacuum*, 80 (2006) 1066.
12. S. Ji, J. An, D.Y. Jang, Y. Jee, J.H. Shim and S.W. Cha, *Curr. Appl. Phys.*, 16 (2016) 324.
13. S. Burinskas, V. Adomonis, V. Žalnierukynas, J. Dudonis and D. Milčius, *Mater. Sci.*, 16(1) (2010) 67.
14. F.C. Fonseca, S. Uhlenbruck, R. Nedéléc and H.P. Buchkremer, *J. Power Sources*, 195 (2010) 1599.
15. S. Sønderby, T. Klemensø, B.H. Christensen, K.P. Almtoft, J. Lu, L.P. Nielsen and P. Eklund, *J.*

Power Sources, 267 (2014) 452.
16. J. Bohlmark, M. Ostbye, M. Lattemann, H. Ljungcrantz, T. Rosell and U. Helmersson, *Thin Solid Films*, 515 (2006) 1928.
17. K. Sarakinos, J. Alami and S. Konstantinidis, *Surf. Coat. Tech.*, 204 (2010) 1661.
18. A.N. Odivanova, V.G. Podkovyrov, N.S. Sochugov and K.V. Oskomov, *Plasma Phys. Rep.*, 37(3) (2011) 239.
19. S. Sønderby, B.H. Christensen, K.P. Almtoft, L.P. Nielsen and P. Eklund, *Surf. Coat. Tech.*, 281 (2015) 150.
20. A.A. Solov'ev, N.S. Sochugov, A.V.Shipilova, K.B. Efimova and A.E. Tumashevskaya, *Russ. J. Electrochem.*, 47(4) (2011) 494.
21. W. Jung, J.L. Hertz and H. Tuller, *Acta Mater.*, 57 (2009) 1399.
22. W. Araki, Y. Imai and T. Adachi, *J. Eur. Ceram. Soc.*, 29 (2009) 2275.
23. J. Ahn, H.W. Jang, H. Ji, H. Kim, K.J. Yoon, J.W. Son, B.K. Kim, H.W. Lee and J.H. Lee, *Nano Lett.*, 18(5) (2018) 2794.
24. N. Schichtel, C. Korte, D. Hesse and J. Janek, *Phys. Chem. Chem. Phys.*, 11 (2009) 3043.
25. J.H. Joo and G.M. Choi, *Solid State Ionics*, 177 (2006) 1053.
26. B.N. Chapman, Glow Discharge Processes: Sputtering and Plasma Etching, John Wiley and Sons, (1980) New York, USA.
27. G. Laukaitis, J. Dudonis and D. Milcius, *Solid State Ionics*, 179 (2008) 66.
28. K. Muthukkumaran, P. Kuppusami, T. Mathews, E. Mohandas and S. Selladurai, *Mater. Sci. Poland*, 25 (2007) 671.
29. I. Riess, M. Gödickemeier and L.J. Gauckler, *Solid State Ionics*, 90 (1996) 91.
30. V. Sivasankaran, L. Combemale, M.C. Pera and G. Caboche, *Fuel Cells*, 14 (2014) 533.